JOURNAL OF SOLID STATE CHEMISTRY 5, 255–261 (1972)

A Mössbauer and ESR Study of $CaO \cdot 6Al_2O_3$–$CaO \cdot 6Fe_2O_3$ Solid Solutions

F. P. GLASSER AND F. W. D. WOODHAMS
University of Aberdeen, Aberdeen, Scotland
AND
R. E. MEADS AND W. G. PARKER
University of Exeter, Exeter, Devon, England

Received November 8, 1971

Mössbauer spectra of $CaAl_{12-x}Fe_xO_{19}$ solid solutions with $x \leqslant 4.8$ show three resolvable quadrupole doublets arising from ferric ions in tetrahedral, trigonal bipyramidal and octahedral sites. Analysis of the relative area ratios shows a marked preference for iron occupation of the tetrahedral sites. Magnetic ordering is observed at 77°K for $x = 4.8$ and 6. An ESR spectrum of $x = 1.2$ is dominated by a $g' = 2$ super-exchange resonance; that of $x = 0.1$ shows a complex pattern attributable mainly from ferric ions in an axially distorted site with zero rhombic distortion.

1. Introduction

Following the discovery of magnetoplumbite by Aminoff (*1*), $PbO \cdot 6Fe_2O_3$ and other isostructural phases have been synthesized. Bertaut (*2*) showed that the trivalent ion could be substituted in whole or in part by Ga^{3+}, Al^{3+} or Cr^{3+}; it had long been known that the Pb^{2+} could be substituted by Ca^{2+}, Sr^{2+} or Ba^{2+}. The crystal structure of magnetoplumbite, $PbO \cdot 6Fe_2O_3$, was determined by Adelskold (*3*) who showed that it consisted essentially of spinel-like blocks separated by layers containing the large divalent ions. Other closely related structures are known. $Na_2O \cdot 11Al_2O_3$ is a representative of the so-called β-Al_2O_3 family which differs from magnetoplumbite mainly in the constitution of the layer which separates the spinel blocks. Another related family appears to contain a smaller divalent ion; Braun (*4*) has described the crystal structures of phases *W*, *X*, *Y* and *Z*. These are related both in chemistry and structure to $BaO \cdot 6Fe_2O_3$ (which is isostructural with magnetoplumbite), but phases *W* and *X* contain a small amount of essential Fe^{2+}, whereas *Y* and *Z* contain Zn^{2+} and Co^{2+}, respectively.

Dayal and Glasser (*5*) showed that $CaO \cdot 6Al_2O_3$ forms solid solutions with a hypothetical iron end member, $CaO \cdot 6Fe_2O_3$, extending to *ca.* 70 mole% of the latter. If prepared under oxidative conditions, the solid solutions are virtually free of Fe^{2+}. Lister and Glasser (*6*) using powder and single-crystal X-ray studies, have shown that the solid solutions have the magnetoplumbite structure. The purpose of the present paper is to explore the distribution of iron atoms in these solid solutions. The iron can occupy five distinct cation sites. Three of these sites afford octahedral coordination and have multiplicities and symmetries, respectively, of two ($\bar{3}m$), four ($3m$) and twelve (m). Four of the irons are tetrahedral ($3m$) and two are coordinated by five oxygens in a trigonal bipyramidal arrangement ($\bar{6}m2$).

Van Loef and Franssen (*7*), van Loef (*8*) and van Wieringen and Rensen (*9*) have interpreted Mössbauer spectra of the isostructural $BaFe_{12}O_{19}$ in terms of the above five sites, but the calcium hexaluminates containing small amounts of iron have not been studied previously.

2. Experimental

Six samples of $CaAl_{12-x}Fe_xO_{19}$ with $x = 6.0$, 4.8, 2.0, 1.2, 0.5 and 0.1 were prepared by firing

mixtures of chemically pure $CaCO_3$, Al_2O_3 and Fe_2O_3 at temperatures between 1300 and 1500°C. At least three sinterings, with intermediate grindings, were required to produce a homogeneous solid solution. The last sintering was done in an air atmosphere at 1300°C to minimize any reduction of Fe^{3+}. The phase purity and homogeneity of each preparation was checked by X-ray powder diffraction, using a Guinier-type focusing camera.

Mössbauer spectra were recorded on a conventional constant acceleration spectrometer using a 400-channel Intertechnique SA43 analyzer operating in multiscaler mode. Spectra were accumulated as mirror images in the first and second 200 channels of the analyzer. The electromechanical drive system was based on a design due to Clark et al. (*10*) with a modified integrator due to Howie (*11*). The source used was ^{57}Co in Pd and the γ-ray detector a xenon–methane proportional counter. Velocity calibration was carried out using metallic Fe foil and the data of Preston et al. (*12*), who give values of 1.677, 6.167 and 10.657 ± 0.025 mm/sec for iron.

Absorbers were prepared by dispersing the sample powder in acrylic discs. The amount of powder in each disc was calculated using Shimony's (*13*) optimization technique which resulted in absorbers containing about 5 mg/cm^2 of natural iron, so that no appreciable thickness broadening effects were expected. The low-temperature spectra were taken with the absorber cooled in a conventional cold-finger vacuum cryostat; the high-temperature spectra, with the absorber in a vacuum furnace similar in design to that described by van der Woude and Boom (*14*). In the latter case the absorber was a thin layer of the sample powder pressed between beryllia discs in a stainless-steel mount.

The ESR spectra were taken at room temperature on a Decca *X*-band spectrometer.

3. Results and Discussion

3.1. Mössbauer Spectra

The Mössbauer spectra of solid solutions with $x \leqslant 4.8$ at room temperature show resonances typical of paramagnetic iron. A representative velocity spectrum, that for $x = 1.2$, is shown in Fig. 1. No appreciable resonance was observed in the $x = 0.1$ compound due to its very low Fe content. There was no significant change in the spectra on cooling to 77°K for compounds with $x \leqslant 2.0$ or in the $x = 2.0$ spectrum on heating to

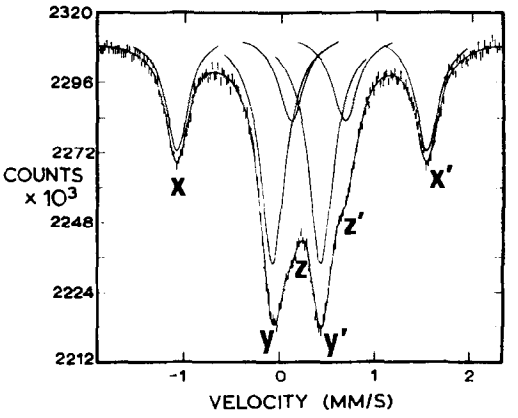

FIG. 1. Mössbauer spectrum of $CaAl_{10.8}Fe_{1.2}O_{19}$ at room temperature. The zero of velocity refers to the centre of the ^{57}Fe calibration spectrum. The solid line is a three-quadrupole doublet least-squares fit to the data.

500°C. Magnetic ordering was observed in the $x = 4.8$ and $x = 6$ samples at 77°K; Fig. 2 shows the velocity spectrum of $x = 4.8$ at 77°K. The room temperature spectrum of $x = 6$ was poorly resolved, typical of a compound close to its magnetic transition temperature.

The paramagnetic spectra show two well resolved doublets XX' and YY' (Fig. 1) with evidence of a third doublet ZZ' superposed on YY'. There was a significant asymmetry of the component lines of the doublets, particularly noticeably for the XX' peaks, of $x = 0.5$ at both room temperature and 77°K. Asymmetry between the component lines of a quadrupole doublet arises from one or more of the following effects: (i) preferential orientation of the microcrystals in the absorber; (ii) Gol'danskii–Karyagin effect, i.e., anisotropy of the recoil-free fraction for atoms in noncubic sites; and (iii) paramagnetic

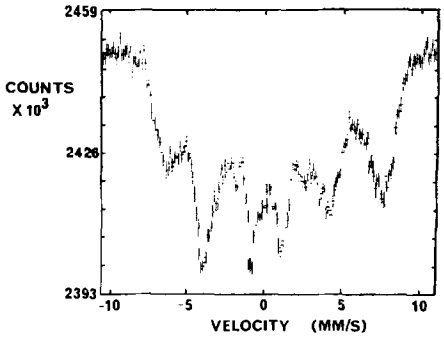

FIG. 2. Mössbauer spectrum of $CaAl_{12.2}Fe_{4.8}O_{19}$ at 77°K.

relaxation effects [see, for example, Wignall (*15*)]. There was no change in the velocity spectrum when the angle between source and absorber was varied, so (i) may be ruled out. The Gol'danskii–Karyagin effect (ii) may be discounted as the asymmetry was observed only in the low iron content, $x = 0.5$ sample. Thus, we believe the asymmetry is due to relaxation effects, the temperature independence of the asymmetry indicating that the dominant electronic relaxation process is spin–spin, and not spin–lattice. Spin–spin relaxation times are expected to decrease with decreasing Fe–Fe separation, leading to a reduction in asymmetry and narrowing of the resonance peaks. This is the case here; the higher Fe content samples show no evidence of asymmetry between the doublet peaks, or any marked line broadening.

The observation of three quadrupole doublets in the spectra is in agreement with the known coordination sites available for Fe occupation in the magnetoplumbite structure. The doublets were identified with the cation sites in the following way. A standard iterative technique least-squares program was used to computer fit the spectra to a three-doublet model. Each pair of doublet lines was constrained to have equal widths and areas, and all lines were assumed to be Lorentzian shaped. No account was taken of the asymmetry of the $x = 0.5$ sample when fitting.

The Mössbauer parameters for the spectra are given in Table I, together with their standard deviations quoted with 95% confidence limits. The parameters are the average for the two mirror image spectra. Isomer shifts are quoted with respect to metallic iron at room temperature.

The isomer shifts of all three doublets are small and fall in the range expected for high-spin ferric ions (Fe^{3+}, ^6S) in oxide environments [see, for example, Bancroft et al. (*16*)]. The quadrupole

TABLE I

MÖSSBAUER PARAMETERS OF $CaAl_{12-x}Fe_xO_{19}$

Sample x	Run No.	Temp.	Site	IS[a]	QS	LW	Fe
0.5	577	R.T.	4	0.186(12)	0.47(4)	0.49(6)	0.61(14)
			5	0.219(16)	2.666(14)	0.33(4)	0.25(5)
			6	0.314(36)	0.78(5)	0.35(10)	0.15(9)
0.5	578	77°K	4	0.26(8)	0.45(18)	0.53(9)	0.49(19)
			5	0.326(6)	2.77(2)	0.46(4)	0.30(8)
			6	0.44(12)	0.68(24)	0.44(10)	0.22(18)
1.2	482	R.T.	4	0.179(4)	0.521(4)	0.33(1)	1.36(10)
			5	0.222(4)	2.650(8)	0.30(2)	0.60(5)
			6	0.419(12)	0.58(1)	0.31(3)	0.46(7)
2.0	185	R.T.	4	0.169(2)	0.551(2)	0.32(1)	1.76(8)
			5	0.244(2)	2.640(5)	0.34(1)	0.84(4)
			6	0.397(5)	0.614(4)	0.40(1)	1.44(8)
2.0	237	500°C	4	0.025(8)	0.554(6)	0.33(2)	1.92(28)
			5	0.039(7)	2.58(2)	0.34(3)	0.68(12)
			6	0.20(2)	0.56(1)	0.39(4)	1.40(32)
2.0	353	77°K	4	0.13(1)	0.55(1)	0.35(2)	1.92(20)
			5	0.20(1)	2.68(2)	0.32(3)	0.80(12)
			6	0.35(1)	0.63(1)	0.40(3)	1.36(24)
4.8	607	R.T.	4	0.181(4)	0.559(4)	0.340(13)	1.19(15)
			5	0.244(6)	2.516(14)	0.31(3)	4.12(30)
			6	0.400(6)	0.631(5)	0.380(14)	4.26(30)

[a] IS, isomer shift with respect to metallic iron at room temperature. To convert to isomer shift scale based on sodium nitroprusside dihydrate add +0.257 mm/sec [Muir et al. (*26*)]; QS, quadrupole splitting; LW, line width; Fe, number of Fe atoms in each site. IS, QS and LW values in mm/sec. Standard deviations in units of last decimal place, e.g., 0.186(12) stands for 0.186 ± 0.012.

splittings of YY' and ZZ' are also small and characteristic of ferric compounds, while that of XX' is much larger falling in the range generally observed for high-spin ferrous ions (Fe^{2+}, ^5D) in a distorted environment. However the small change in the XX' quadrupole splitting with temperature, combined with its small isomer shift, together with a knowledge of the oxygen environments around each of the three cation sites all point to the fact that XX' arises from ferric ions in a very distorted site, probably the trigonal bipyramid ($\bar{6}m2$) site at the junction of the Ca–O layer and the spinel block. Quadrupole splittings of this order have also been observed at the trigonal bipyramidal site in $BaFe_{12}O_{19}$ (*8*, *9* and present authors) and at five-coordinate iron sites in organic compounds (*17*).

The remaining doublets YY' and ZZ' must then arise from iron ions in the octahedral Fe(VI) and tetrahedral Fe(IV) sites. Bancroft et al. (*16*) and Edwards et al. (*18*) have shown that isomer shifts generally decrease with decreasing coordination number and on this basis we assign YY' to Fe(IV) and ZZ' to Fe(VI). The isomer shift of XX', the five-coordinate site Fe(V) absorption, then lies between those of Fe(IV) and Fe(VI). The increase in isomer shifts with decreasing temperature is of the order expected by the second-order Doppler effect.

The linewidths of the solid solution with $x > 0.5$ of the Fe(IV) and Fe(V) doublets are only broadened slightly compared to the value of 0.23 mm/sec obtained with a natural iron absorber. This small degree of broadening probably reflects a slight spread of electric field gradients at the iron ions due to a statistical fluctuation of Fe and Al ions on neighbouring cation sites. The linewidths of the Fe(VI) doublets are, however, considerably broadened reflecting the fact that there is not a single unique octahedral site, but three crystallographically distinct octahedral sites. These sites are not sufficiently different to give three resolvable doublets; instead a single doublet with line broadening is observed. Line broadening was much greater for the $x = 0.5$ sample due probably, as discussed earlier, to electron spin–spin relaxation effects[1].

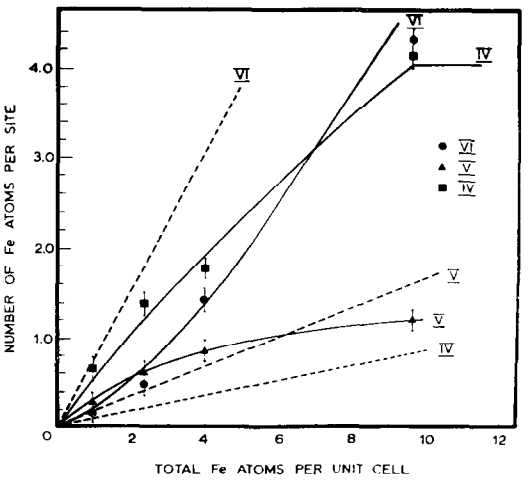

FIG. 3. Site occupancy of Fe atoms in $CaAl_{12-x}Fe_xO_{19}$. IV, V, VI refer to the tetrahedral, trigonal bipyramid and octahedral sites, respectively. The unit cell contains two formula units.

The number of iron atoms in each of the three sites was determined directly from the area ratios of the doublets on the assumptions that the recoil-free fractions of the sites are equal and that there were no thickness broadening effects. Sawatzky et al. (*17*) have shown that the ratio of the recoil-free fractions of ^{57}Fe in the octahedral and tetrahedral sites in Fe_3O_4 at room temperature is 0.94 ± 0.02, i.e., close to unity, so that our assumption of equal recoil-free fractions is not too unreasonable. No significant absorber thickness effects were expected as the absorbers were deliberately kept thin. The number of iron atoms in each site is given in Table I and the results plotted graphically in Fig. 3. The broken lines show the expected site occupations on the basis of a random-model filling. The results show that there is a marked preference for the tetrahedral, Fe(IV), sites and at $x = 4.8$ this site is completely occupied by iron ions. The occupation of the Fe(V) sites is close to random while that of the Fe(VI) sites is significantly less than that given by the random model, although of course for values of x greater than about 4.5 the octahedral site must become the dominant iron site. No distinction has been made between the three slightly different octahedral sites.

[1] Rensen and Wieringen (*19*) have recently interpreted single-crystal variable temperature Mössbauer spectra of $BaFe_{12}O_{19}$ below the Curie temperature as showing that the recoil-free fractions of the FeV site is strongly asymmetric due to the Fe ions having a much larger thermal motion in the direction of the c axis than perpendicular to it. Above the Curie temperature this should give rise to a marked Gol'danskii–Karyagin effect: such an effect was quantitatively found (*9*). Similar effects were not observed in the present experiments and it is concluded that any asymmetry in the thermal motion of Fe(V) perpendicular and parallel to the c axis is small.

3.2. Electron Spin Resonance Spectra

3.2.1. Introduction

X-band ESR spectra of $CaAl_{12-x}Fe_xO_{19}$ samples with $x = 1.2$ and $x = 0.1$ Fe^{3+} are shown in Figs. 4a and 4b. The high iron concentration spectrum is dominated by a broad $g' = 2$ resonance, typical of transitions between levels of a super-exchange multiplet due to Fe^{3+} ions in adjacent cation sites. As the iron concentration is lowered other features appear and at the lowest concentration studied, $x = 0.1$, a complex pattern of relatively sharp resonances is observed.

The powder ESR spectrum of high spin Fe^{3+} has been discussed by a number of workers; see, for example, Castner et al. (*21*), Wickman et al. (*22*) and Blumberg (*23*). The appropriate spin Hamiltonian is:

$$\mathcal{H} = g\beta\mathbf{H}\cdot\mathbf{S} + D[S_z^2 + \tfrac{1}{3}S(S+1)] + E(S_x^2 - S_y^2)$$

where D and E are the crystal field terms, S_x, S_y and S_z are components of spin along three mutually perpendicular crystalline axes (chosen so that no crossterms such as S_xS_y occur in $\mathcal{H}$), $g = 2$, H the static applied field and β the Bohr magneton. For Fe^{3+}, $S = \frac{5}{2}$ calculation of the eigenvalues involves diagonalization of a 6×6 matrix. If $H = 0$ and $E = 0$ the axial crystal field term D results in three degenerate doublets corresponding to $S_z = \pm\frac{5}{2}$, $\pm\frac{3}{2}$ and $\pm\frac{1}{2}$. The inclusion of the rhombic term E results in mixing of the states, which are further split by the magnetic field. An axial crystal field corresponds to the case $E = 0$. Increasing rhombic character is commonly expressed by use of the parameter $\lambda = E/D$. Blumberg (*23*) has shown that maximum rhombic distortion corresponds to the case where $\lambda = \frac{1}{3}$. Observable resonances in powders are obtained only when the value of resonant energy, which is dependent on the angles between the magnetic field and the principal axes of the crystal field tensor, passes through stationary values. This situation arises for crystal orientations in which the magnetic field lies along the x, y or z principal axis or is in the xy, xz or yz plane.

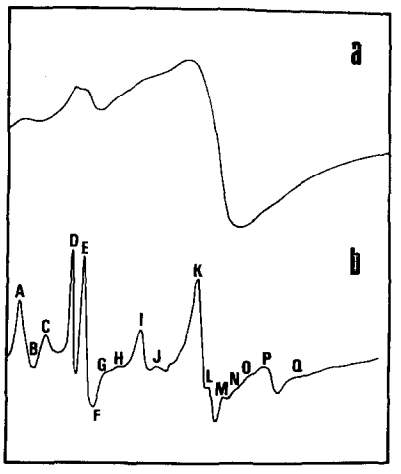

FIG. 4. ESR spectra recorded at *X*-band frequency (9.2 GHz) of $CaAl_{12-x}Fe_xO_{19}$ for (a) $x = 1.2$ and (b) $x = 0.1$. The ordinate represents the first derivative of the microwave power absorption, in arbitrary units.

Extensive computations of energies expected for powder resonances have been made by Gibson and coworkers [see Dowsing and Gibson (*24*)] and by Aasa (*25*). Much use has been made in interpreting the present data, of these computations, presented graphically by the authors. The format of presentation varies somewhat from author to author; we shall adopt that of Aasa. In his graphs the values of g/g' (g' = the effective g value of the resonance given by $g'\beta H = h\nu$) are plotted as a function of $h\nu/D$, where $h\nu$ is the microwave quantum energy. At *X*-band (9.2 GHz) this corresponds to a wave number of 0.326 cm^{-1}. Such graphs are plotted for various values of λ for each of the transitions between adjacent states, labeled in increasing energy order 1 to 6. Other possible transitions are not included in Aasa's calculations.

Interpretation of the resonance spectrum of Fe^{3+} in $Ca_2Al_{24-x}Fe_xO_{38}$ is rendered difficult by the following:

(i) Uncertainty in the value of g' to be attributed to a given resonance in the experimental spectrum owing to uncertainty in line shape. The line shape will depend in detail on the manner in which the resonance energy varies with angle near the stationary value.

(ii) the large number of resonance lines observed, the complexity of the spectrum and the lack of detailed information on relative intensities at present available makes site assignment characterized by values of D and λ difficult to do unambiguously. The following interpretation must therefore be regarded as somewhat tentative.

3.2.2. Interpretation of the Spectrum

Detailed analysis of the $x = 0.1$ spectrum (Fig. 4b) has been carried out and the measured g' values and line identifications are given in

Table II. The following conclusions have been made.

(i) The well known resonance at $g' = 4.27$ corresponding to an Fe^{3+} site of high rhombic distortion ($\lambda = \frac{1}{3}$) is not present to any significant extent. The occurrence of strong resonances in the $g' = 6$ and $g' = 2$ regions is characteristic of sites with low values of λ (i.e., axial symmetry).

(ii) The strong resonance D at $g' = 6.1$ can arise from transitions $1 \rightarrow 2$ and $3 \rightarrow 4$ for λ near zero and for small values of $h\nu/D$. The occurrence of an intense doublet including the line E at $g' = 5.2$ suggests however a higher value of $h\nu/D$ in which case the resonance due to transition $1 \rightarrow 2$ moves to lower g' values. A low field expansion of the spectrum reveals a doublet structure, lines A and B, near $g' = 20$. This is consistent with $h\nu/D$ values between about 1.7 and 3.5 for transitions $2 \rightarrow 3$ and $4 \rightarrow 5$. A reasonably complete interpretation of most of the intense resonances in terms of one site can be obtained by assuming $h\nu/D$ is near 1.7 and $\lambda = 0$. The positions of the expected resonances g'_{calc} for this site, site 1, are given in Table II.

(iii) The resonances at $g' = 3.1$ (I), $g' = 2.7$ (J) and $g' = 2.2$ (K) are not well fitted by the assumptions of site 1. They can be plausibly interpreted in terms of a second site 2 for which $h\nu/D = 0.6$ and $\lambda \simeq 0.15$. This also fits the resonance P at $g' = 1.64$ and provides contributions to, or alternative assignments for resonances C and E.

(iv) As an alternative to, or possibly in addition to site 2, the assumption of site 2′ with $h\nu/D \simeq 12$ and $\lambda = 0$ provides another explanation of resonances K and P, and also interprets resonances M, N and O.

(v) Low field expansion suggests that the resonance F ($g' = 4.8$) is genuine. This, together with other weak resonances at $g' = 4.0$ (G) and

TABLE II

ESR PARAMETERS FOR $CaAl_{11.9}Fe_{0.1}O_{19}$

Resonance[a]	Intensity	g'	g/g'	H (Oe)	Site 1 g/g'_{calc}	Site 1 Transition	Site 2 g/g'_{calc}	Site 2 Transition	Site 2 g/g'_{calc}	Site 2 Transition	Site 3 g/g'_{calc}	Site 3 Transition
A	***	24.1	0.08	280	0.08	$2 \rightarrow 3z$						
B	***	17.9	0.11	370	0.12	$2 \rightarrow 3x,y$						
C	**	9.3	0.22	720	0.21	$5 \rightarrow 6z$	0.22 0.21	$1 \rightarrow 2y$ $5 \rightarrow 6z$			0.21 0.21	$1 \rightarrow 2y$ $5 \rightarrow 6z$
D	****	6.1	0.33	1090	0.31 0.33	$4 \rightarrow 5z$ $3 \rightarrow 4z$						
E	****	5.2	0.39	1290	0.40 0.40	$1 \rightarrow 2x,y$ $2 \rightarrow 3x,y$	0.37	$3 \rightarrow 4z$				
F	*	4.8	0.41	1380							~0.40	$3 \rightarrow 4z$
G	*	4.0	0.50	1650							~0.50	$3 \rightarrow 4x,z$
H	*	3.7	0.55	1820							~0.55	$3 \rightarrow 4y$
I	***	3.1	0.65	2170			0.65	$3 \rightarrow 4x$				
									0.70	$5 \rightarrow 6z$		
J	**	3.7	0.74	2440			0.75	$1 \rightarrow 2x$				
					0.81	$3 \rightarrow 4z$			0.82	$4 \rightarrow 5z$		
K	****	2.20	0.91	3020			0.90	$3 \rightarrow 4y$	0.90	$1 \rightarrow 2x,y$		
									0.91	$2 \rightarrow 3x,y$		
L	***	2.09	0.96	3180	0.95	$3 \rightarrow 4x,y$						
M	**	1.97	1.02	3370					1.00	$3 \rightarrow 4x,y,z$		
N	*	1.88	1.06	3530	1.09	$2 \rightarrow 3z$			1.09	$4 \rightarrow 5x,y$		
O	*	1.76	1.14	3870					1.15	$5 \rightarrow 6x,y$		
P	***	1.64	1.22	4050	1.25	$2 \rightarrow 3z$	1.22	$3 \rightarrow 4y$	1.22	$1 \rightarrow 2z$		
Q	*	1.48	1.35	4490			1.45	$2 \rightarrow 3y$	1.22	$2 \rightarrow 3z$	~1.3–1.4	$1 \rightarrow 2x$
							1.47	$4 \rightarrow 5z$				

[a] Resonances A–Q refer to Fig. 4b; Intensity, **** strong, *** medium, ** weak, * very weak; g', measured g-value; H, value of magnetic field giving rise to resonance.

$g' = 3.7$ (H) may constitute the $g' \simeq 4$ triplet expected for higher values of λ in a site which, in this material, has low Fe^{3+} population. The parameters (site 3) giving a good fit are $h\nu/D < 1$ and $\lambda = 0.23$–0.24.

To summarize, a fairly complete understanding can be made of the ESR spectrum, on the assumption of three or probably four sites, with the following parameters:

Site	$h\nu/D$	D (cm^{-1})	λ
1	1.7	0.19	0
2	0.6	0.54	0.15
2′	12	0.03	0
3	<1	>0.3	0.23

The Mössbauer spectra of the higher Fe concentration samples show a preferential occupation of the tetrahedral iron site in calcium hexaluminate. If this is also true for the $x = 0.1$ sample, it is plausible to assume that site 1 is identified with the Fe(IV) site which must, since $\lambda = 0$, have axial symmetry suggesting the point group C_{3v}...$3m$.

4. Conclusions

Mössbauer spectra of samples of $CaAl_{12-x}Fe_xO_{19}$ with $x \leqslant 4.8$ show three resolvable quadrupole doublets at room temperature. These doublets are attributed to high-spin Fe^{3+} ions in the tetrahedral, trigonal bipyramidal and octahedral cation sites of the crystal structure. The quadrupole splitting of the five-coordinate site is believed to be one of the largest reported to date for a high-spin ferric ion, and reflects the large distortion of the site. Analysis of the area ratios of the doublets show a marked preference of Fe^{3+} for the tetrahedral sites. Magnetic ordering was observed in the 77°K spectra of $x = 6$ and $x = 4.8$. These spectra are complicated due to the presence of (at least) three unique ferric sites and have not yet been analyzed in detail.

Electron spin resonance spectra were taken of samples with $x = 1.2$ and $x = 0.1$ at X-band frequency. The spectrum of $x = 1.2$ is dominated by a broad super-exchange $g' = 2$ resonance; that of $x = 0.1$ shows a complex pattern of sharp lines. The majority of these resonances may be interpreted as due to Fe^{3+} ions in an axially distorted site but with zero rhombic distortion. The remaining weaker resonances are attributed to a further two, and possibly three, Fe^{3+} sites.

5. Acknowledgments

Thanks are due to Dr. J. E. Cousins, Mr. C. S. Bowring and Mr. M. Hardiman for the use and operation of the ESR spectrometer.

References

1. G. Aminoff, *Geol. Foenren Stockholm Foerh.* **47**, 283 (1925).
2. F. Bertaut, A. Deschamps, R. Pauthenet, and S. Pickart, *J. Phys. Radium* **20**, 404 (1959).
3. V. Adelsköld, *Arkiv Kemi Mineral. Geol.* **12A**, 1 (1938).
4. P. B. Braun, *Philips Res. Rep.* **12**, 491 (1957).
5. R. R. Dayal and F. P. Glasser, *Science of Ceramics*, pp. 191–214. Academic Press, New York (1967).
6. D. H. Lister and F. P. Glasser, *Trans. Brit. Ceram. Soc.* **66** (7), 293 (1967).
7. J. J. van Loef and P. J. M. Franssen, *Phys. Lett.* **7**, 225 (1963).
8. J. J. van Loef, *Physica* **32**, 2102 (1966).
9. J. S. van Wieringen and J. G. Rensen, *Z. Angew. Phys.* **21**, 69 (1966).
10. P. E. Clark, A. W. Nichol, and J. S. Carlow, *J. Sci. Instrum.* **44**, 1001.
11. I. Howie, private communication. Copies of the circuit diagrams are available from F. W. D. W.
12. R. S. Preston, S. S. Hanna, and J. Heberle, *Phys. Rev.* **128**, 2207 (1962).
13. V. Shimony, *Nucl. Instr. Meth.* **37**, 348 (1965).
14. F. van der Woude and G. Boom, *Rev. Sci. Instrum.* **36**, 800 (1965).
15. J. W. G. Wignall, *J. Chem. Phys.* **44**, 2462 (1966).
16. G. M. Bancroft, A. G. Maddock, and R. G. Burns, *Geochim. Cosmochim. Acta* **3**, 2219 (1967).
17. E. de Boer, L. K. de Vries, and J. M. Trooster, *Inorg. Chem.* **10**, 81 (1971).
18. P. R. Edwards, C. E. Johnson, and R. J. P. Williams, *J. Chem. Phys.* **47**, 2074 (1967).
19. J. G. Rensen and J. S. van Wieringen, *Solid State Commun.* **7**, 1139 (1969).
20. G. A. Sawatzky, F. van der Woude, and A. H. Morrish, *Phys. Rev.* **183**, 383.
21. T. Castner, Jr., G. S. Newell, W. C. Holton, and C. P. Slichter, *J. Chem. Phys.* **32**, 668 (1960).
22. H. H. Wickman, M. P. Klein, and D. A. Shirley, *J. Chem. Phys.* **42**, 2113 (1965).
23. W. E. Blumberg, *in* "Magnetic Resonance in Biological Systems." Proceedings 2nd International Conference, Stockholm, 1966. (A. Ehrenberg, B. G. Malmström and T. Warngard, Eds.), Pergamon, Elmsford, NY (1967).
24. R. D. Dowsing and J. F. Gibson, *J. Chem. Phys.* **50**, 294 (1969).
25. R. Aasa, *J. Chem. Phys.* **52**, 3919 (1970).
26. A. H. Muir, Jr., K. J. Ando, and H. M. Coogan, "Mössbauer Effect Data Index, 1958–1965," p. 26. Interscience, New York (1967).